Department of Electrical and Computer Systems Engineering

Technical Report MECSE-22-2004

NOLM-NALM Fiber Ring Laser

W. J. Lai, P. Shum and L.N. Binh

MONASH UNIVERSITY

NOLM-NALM Fiber Ring Laser

W. J. Lai, *Student Member, IEEE*, P. Shum, *Member, IEEE*, L. N. Binh

***Abstract*— We study the bidirectional lightwave propagation in an erbium doped fiber ring laser and its observed optical bistability behavior. We develop a model for the inverted-S fiber ring laser using NOLM-NALM principle, which operates in the nonlinear region. Good agreements between the laser experimental performance and the developed model are achieved. Not only the laser shows good switching capability, it also presents the pulse compression feature.**

In addition, the laser model shows the route to chaotic operation via period doubling bifurcation, when the input power increases. However, experimentally we only obtain the quasi-periodic operation when it is amplitude modulated, due to constraint of photonic components. Nevertheless, we foresee the possibility of the chaotic operation of the laser.

***Index Terms*— Optical fiber lasers, mode-locked lasers, bifurcations, optical bistability, optical switching**

I. Introduction

Fiber ring laser is a rich and active research field in optical communications. Many fiber ring laser configurations have been proposed and constructed to achieve different objectives. It can be designed for cw (continuous wave) or pulse operation; linear or nonlinear operation; fast or slow repetition rate; narrow or broad pulse width etc; for various kinds of photonic applications.

The simplest fiber laser structure shall be an optical closed loop with a gain medium, and some associated optical components such as optical couplers. The gain medium used can be any rare earth element doped fiber amplifier, semiconductor optical amplifier, parametric amplifier, etc; as long as it provides the gain requirement for lasing. Without any mode-locking mechanism, the laser shall operate in the cw regime. By inserting an active mode-locker [5,7-8], i.e. amplitude or phase modulator, the resulting output shall be an optical pulse train operating at the modulating frequency, when the phase conditions is matched. This often results in a high-speed optical pulse train, however with broad pulse width. There is another kind of fiber laser, which uses the nonlinear effect in generating the optical pulses, and is known as the passive mode-locking technique. Saturable absorber, stretched pulse mode-locking [10], nonlinear polarization rotation [9], figure-eight fiber ring lasers [5], etc are grouped under this category. This type of laser generates a shorter optical pulse in exchange of the repetition frequency. Hence, this is the trade off between the active and passive mode-locked systems. Fiber ring lasers are often very sensitive to the environmental effects, such as temperature change, mechanical vibration, polarization drift and etc. Hence, there are many techniques have been demonstrated to improve the laser stability. Just to name a few: regenerative active mode-locked fiber ting laser [6], all polarization-maintaining configuration [8], cavity length adjustment via piezo-electric transducer (PZT), etc.

Although there are different types of fiber laser, with different operating regimes and operating principles, one common criterion is the uni-directionality, besides the gain and phase matching conditions. Uni-directional operation has been proved to offer better lasing efficiency, less sensitive to back reflections and good potential for single longitudinal mode operation [1], and can be achieved by incorporating an optical isolator within the laser cavity. [2] has demonstrated a unidirectional inverted S-type erbium doped fiber ring laser without the use of optical isolator, but with optical couplers. In their laser system, the lightwaves are passed through in one direction and suppressed in the other using certain coupling ratios, hence, achieving unidirectional operation. However, only the power difference between the two cw (continuous wave) lightwaves was studied, and the works did not extend further into unconventional and nonlinear regions of operation.

In this paper, we study the bidirectional lightwave propagation in an erbium doped fiber ring laser and observe the optical bistability behavior. We then exploit this commonly known as undesirable bidirectional lightwave propagation in constructing a kind of fiber laser configuration based on nonlinear optical loop mirror (NOLM) and nonlinear amplifying loop mirror (NALM) structure. This laser configuration is similar to the one demonstrated by [2], however, we operate the laser in different regions of the operation. We investigate the switching capability of the laser basing on its bistability behavior. Furthermore, we focus on the nonlinear dynamics of the constructed laser, and observed some optical bifurcation phenomenon.

In Section II, the operation principles of the nonlinear optical loop mirror (NOLM) and nonlinear amplifying loop mirror (NALM) are briefly discussed. Section III describes the formulation of the NOLM-NALM fiber ring laser. Section IV gives the experimental setup of our work. Section V presents and discusses the results obtained from the experiment and simulation. Finally, Section VI gives some concluding remarks and possible future developments.

This work was supported in part by the Nanyang Technological Research Fund.

W. J. Lai and P. Shum are with Network Technology Research Centre, Nanyang Technological University, Singapore (phone: 65-67905363; fax: 65-67926894; e-mail: wennjing@pmail.ntu.edu.sg).

L. N. Binh, is with Monash University, Victoria, Australia (e-mail: le.nguyen.binh@eng.monash.edu.au).

II. Nonlinear Optical Loop Mirror & Nonlinear Amplifying Loop Mirror

The operation principles of nonlinear optical loop mirror (NOLM) and nonlinear amplifying loop mirror (NALM) have been studied by [3] and [4]. Here, we will briefly discuss the basic operation of the structures. Both of the structures are very similar to each other, however with an additional gain element in NALM. Also, both of them are operating based on the nonlinear phase shift induced by self phase modulation (SPM). The schematic diagrams of the NOLM and NALM are shown below, with κ is the coupling ratio of the coupler, L is the loop length and G is the gain of the amplifying medium in NALM. The input signal, E_1, is split into two counter propagating fields, E_3 and E_4, which return in coincidence to recombine at the coupler. The optical path lengths experienced by the two propagating fields are exactly the same, since they follow the same route but in opposite directions.

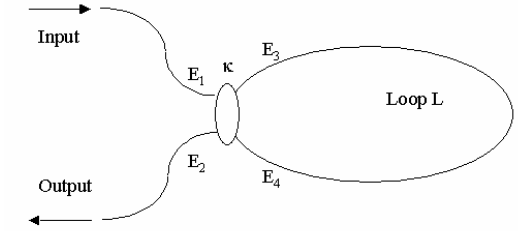

a)

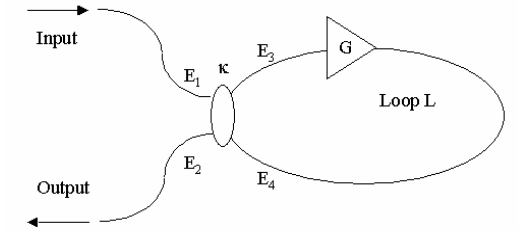

b)

Fig. 1: a) Nonlinear optical loop mirror; b) nonlinear amplifying loop mirror

Under lossless condition, the input-output relationships of a coupler with coupling ratio of κ are [3]

$$E_3 = \sqrt{\kappa}E_1 + j\sqrt{(1-\kappa)}E_2 \quad (1a)$$

$$E_4 = \sqrt{\kappa}E_2 + j\sqrt{(1-\kappa)}E_1 \quad (1b)$$

with E_1, E_2, E_3 and E_4 assignments shown in Fig. 1. After L propagation, the output signals, E_{3L} and E_{4L} become as follow with nonlinear phase shifts taken into account:

$$E_{3L} = E_3 \exp(j2\pi n_2|E_3|^2L/\lambda) \quad (2a)$$

$$E_{4L} = E_3 \exp(j2\pi n_2|E_4|^2L/\lambda) \quad (2b)$$

Where,

$$|E_3|^2 = \kappa|E_1|^2 + (1-\kappa)|E_2|^2 + j\sqrt{\kappa(1-\kappa)}(E_1^*E_2 - E_2^*E_1)$$

$$= \kappa|E_{01}|^2 + (1-\kappa)|E_{02}|^2 - 2\sqrt{\kappa(1-\kappa)}\,E_{01}E_{02}\sin[(\omega_2-\omega_1)t] \quad (3a)$$

$$|E_4|^2 = \kappa|E_2|^2 + (1-\kappa)|E_1|^2 + j\sqrt{\kappa(1-\kappa)}(E_2^*E_1 - E_1^*E_2)$$

$$= \kappa|E_{02}|^2 + (1-\kappa)|E_{01}|^2 + 2\sqrt{\kappa(1-\kappa)}\,E_{01}E_{02}\sin[(\omega_2-\omega_1)t] \quad (3b)$$

with $E_1 = E_{01}\exp(j\omega_1 t)$ and $E_2 = E_{02}\exp(j\omega_2 t)$.

The last term of (3a) and (3b) is the interference pattern between E_1 and E_2. For simplicity, we assume the input is injected into port 1, i.e. $E_2 = 0$, the resultant E_{3L} and E_{4L} become [3]:

$$E_{3L} = \sqrt{\kappa}E_1 \exp(j\kappa 2\pi n_2|E_1|^2L/\lambda) \quad (4a)$$

$$E_{4L} = j\sqrt{(1-\kappa)}E_1 \exp(j(1-\kappa)2\pi n_2|E_1|^2L/\lambda) \quad (4b)$$

The outputs at port 1 and 2 are:

$$|E_{o1}|^2 = |E_1|^2(2\kappa(1-\kappa)\{1+\cos[(1-2\kappa)2\pi n_2|E_1|^2L/\lambda]\}) \quad (5a)$$

$$|E_{o2}|^2 = |E_1|^2(1-2\kappa(1-\kappa)\{1+\cos[(1-2\kappa)2\pi n_2|E_1|^2L/\lambda]\}) \quad (5b)$$

where n_2 is the nonlinear coefficient, L is the loop length, λ is the operating wavelength. When $\kappa = 0.5$, all the injected power at port 1 will be reflected back to port 1, and no output will appear at port 2, acts on it names.

NALM is an improved exploitation of NOLM. For NALM configuration, a gain medium with gain coefficient, g is added to increase the asymmetric nonlinearity within the loop. The amplifier is placed at one end of the loop, closer to port 3 of the coupler, and is assumed short relative to the total loop length. Hence, the nonlinear phase shift for E_{3L} and E_{4L} can be written as [4]:

$$\theta_{3L} = \kappa g 2\pi n_2|E_1|^2L/\lambda \quad (6a)$$

$$\theta_{4L} = (1-\kappa)2\pi n_2|E_1|^2L/\lambda \quad (6b)$$

The outputs at port 1 and 2 are then:

$$|E_{o1}|^2 = g|E_1|^2(2\kappa(1-\kappa)\{1+\cos[(1-\kappa-g\kappa)2\pi n_2|E_1|^2L/\lambda]\}) \quad (7a)$$

$$|E_{o2}|^2 = g|E_1|^2(1-2\kappa(1-\kappa)\{1+\cos[(1-\kappa-g\kappa)2\pi n_2|E_1|^2L/\lambda]\}) \quad (7b)$$

III. NOLM – NALM Fiber Ring Laser

The configuration of NOLM-NALM fiber ring laser is shown in Fig. 2. It is simply a coupled loop mirrors, with NOLM (ABCEA) on one side and NALM (CDAEC) on the other side of the laser, with a common path in the middle section.

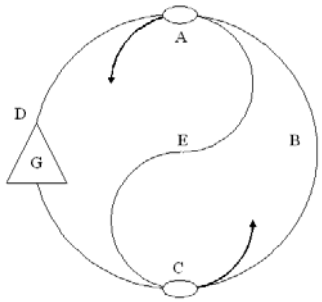

Fig. 2: NOLM-NALM fiber ring laser

We numerically simulate the laser behavior by combining the effects described in the previous section, and obtain the bifurcation maps as shown in Fig. 3, with $\kappa_1 = 0.55$ and $\kappa_2 = 0.65$; L_a, L_b and L_c are 20m, 100m and 20m respectively; nonlinear coefficient of $3.2\text{x}10^{-20}\text{m}^2/\text{W}$; gain coefficient of 0.4/m and operate at 1550nm. κ_1 and κ_2 are the coupling ratio of couplers at point A and C respectively; L_a, L_b and L_c are the fiber length of left, mid and right arm of the leaser cavity. The maps are obtained with 200 iterations.

As a matter of fact that the complex systems tend to encounter bifurcations, which when amplified, can lead to either order or to chaos. Small system perturbations can be iterated to a size that will result in a bifurcation. Bifurcations can be considered as critical points in system

transitions. The points can be cascaded toward chaos, through period doubling; or stabilized in a new behavior through a series of feedback loops, so that the system is in harmony with its environment again.

From the maps obtained, under this system configuration setting, there are three operation regions within this NOLM-NALM fiber ring laser. The first is the linear operation region (0<P<6W), where there are single-value outputs, and they increase with the input power. Period doubling effect starts to appear when the input power reaches ~6W. This is the second operation region (6≤P<8W) of the laser, where double-periodic and quasi-periodic signals can be found here. When the input power goes beyond 8W, the laser will enter into the chaotic state of the operation. The Poincare map of the above system configuration with high pump power is shown in Fig. 4. It shows the pattern of attractor of the system when the laser is operating in the chaotic region.

a)

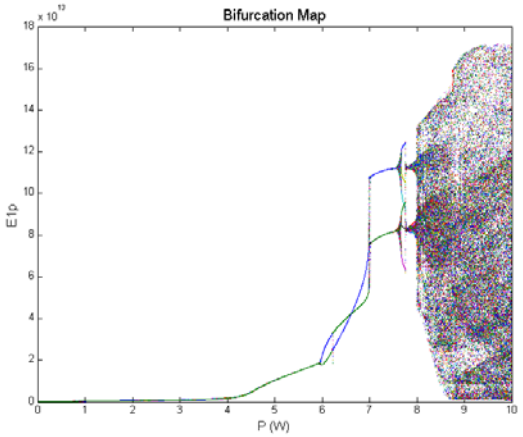

b)

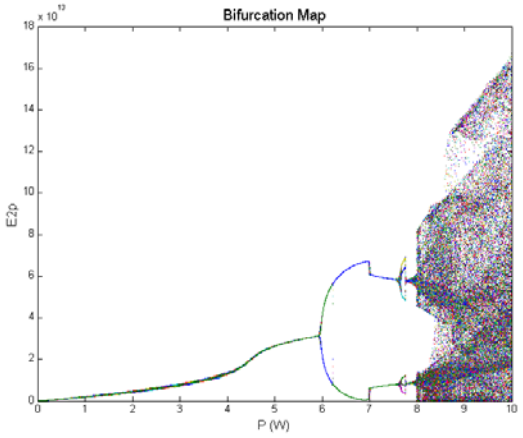

Fig. 3: Bifurcation maps for a) E_1; and b) E_2 with $\kappa_1 = 0.55$ and $\kappa_2 = 0.65$

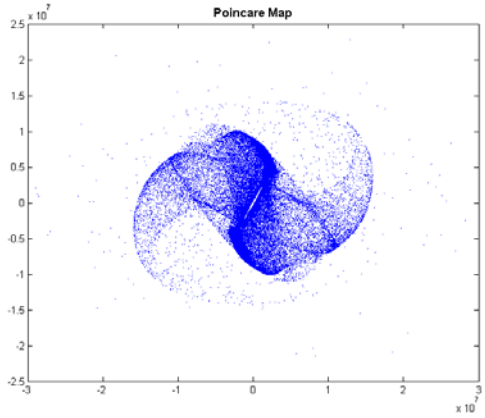

Fig. 4: Poincare map of the system with high pump power with $\kappa_1 = 0.55$ and $\kappa_2 = 0.65$.

By setting $\kappa_2 = 0$, the laser will behave like a NOLM. With an input pulse to port 1 of coupler A and we observe pulse compression at its port 2, as shown in Fig. 5. Fig. 6 presents the transmission capability of the setup at port 2 for various κ_1 values, when the input is injected to port 1 and $\kappa_2 = 0$. When $\kappa_1 = 0.5$, we observe no transmission at port 2, as the entire injected signal has been reflected back to port 1, where the mirror effect takes place. By changing the coupling ratio of κ_2, we are able to change the zero transmission point away from κ_1 =0.50. Fig. 7 shows the transmisivity of Output 1 and Output 2 for various sets of κ_1 and κ_2, where Output 1 is the output port of coupler A, and Output 2 is the output port of coupler C. The figure shows the complex switching dynamics of the laser for different sets of κ_1-κ_2, also with the pulse compression capability.

a) b)

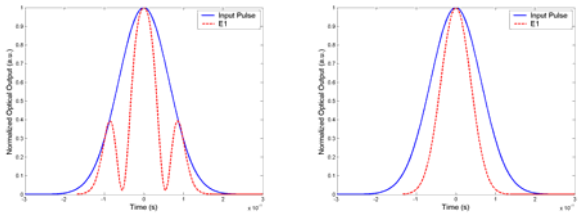

Fig. 5: Input and output pulse at port1 and port 2 comparison with κ_2 = 0and (a) $\kappa_1 = 0.41$ and (b) $\kappa_1 = 0.49$ (solid line – input pulse, dotted line – output pulse at port 1)

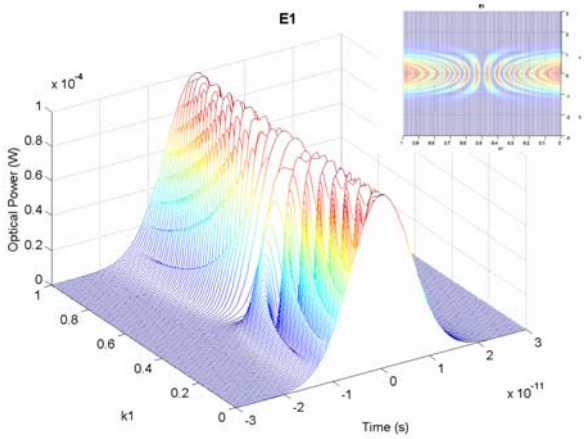

Fig. 6: Output pulse behavior for various κ_1 values, when $\kappa_2 = 0$ for small input power (Inset: top view of the pulse behavior)

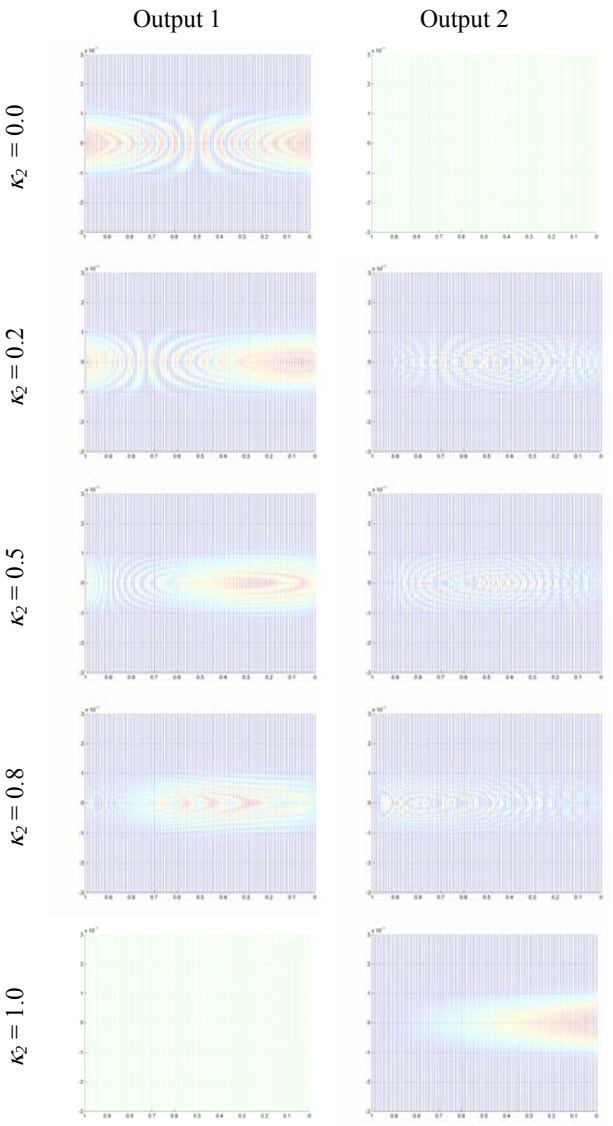

Fig. 7: Intensity plot of output 1 and output 2 for different κ_2 values. (y-axis is intensity of the output pulse, x-axis is the values of κ_1)

IV. Experimental Setup

A. Bidirectional Erbium Doped Fiber Ring Laser

We start with a simple erbium doped fiber ring laser; an optical closed loop with EDFA and some fiber couplers. It is used to study the bi-directional lightwave propagations behavior of the laser. The EDFA is made of a 20m erbium doped fiber (EDF), and dual pumped by 980 and 1480 nm diode lasers, with saturation power of about 15dBm. No isolator and filter is used in the setup to eliminate the direction and spectra constraints. Two outputs are taken for examinations, i.e. Output 1 in counter clockwise direction, and Output 2 in clockwise direction.

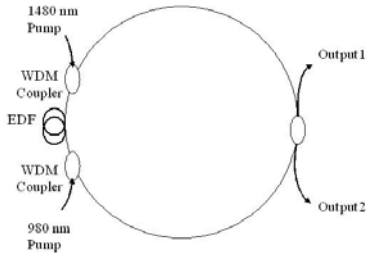

Fig. 8: Experimental setup for erbium doped fiber ring laser

B. NOLM-NALM Fiber Ring Laser

The experimental setup of the NOLM-NALM fiber ring laser is shown in Fig. 9. It is simply a combination of NOLM on one side and NALM on the other side of the laser, with a common path in the middle section. The principal element of the laser is an optical close loop with an optical gain medium, two variable ratio couplers (VRC), an optical bandpass filter (BPF), optical couplers and other associated optics. The gain medium used in our fiber laser system is the amplifier used in the preceding experiment. The two VRCs, with coupling ratios ranging from 20% to 80% and insertion loss of about 0.2dB are added into the cavity at positions shown in the figure to adjust the coupling power within the laser. They are interconnected in such a way that the output of one VRC is the input of the other one. A tunable bandpass filter with 3dB bandwidth of 1 nm at 1555 nm is inserted into the cavity to select the operating wavelength of the generated signal and to reduce the noise in the system. One thing to note is that the lightwave is traveling in both directions, as there is no isolator is used in the laser. Output1 and Output2 as shown in the figure are taken out and analyzed as the outputs of the laser.

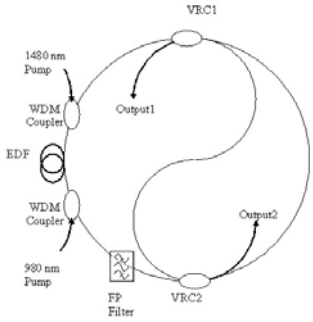

Fig. 9: Experimental setup for NOLM-NALM fiber ring laser

C. AM Modulated NOLM-NALM Fiber Ring Laser

The schematic of AM modulated NOLM-NALM fiber ring laser is shown in Fig. 10. A few new photonic components are added into the laser cavity. An asymmetric coplanar traveling wave 10Gb/s, Ti:$LiNbO_3$ Mach-Zehnder amplitude modulator is also used in the inner loop of the cavity with half wave voltage, V_π of 5.3 V. The modulator is DC biased near the quadrature point and not driven higher than V_π such that it operates on the linear region of its characteristic curve and to ensure minimum chirp imposing on the modulated lightwaves. It is driven by the sinusoidal signal derived from an Anritsu 68347C Synthesizer Signal Generator. The modulating depth is < 1 to avoid signal

distortion. The modulator has an insertion loss of ≤ 7dB. Two polarization controllers are placed prior to the inputs of the modulator in both directions to ensure proper polarization alignment into the modulator. A wider bandwidth tunable FP filter is used in this case to allow more longitudinal modes within the laser for possible mode-locking process.

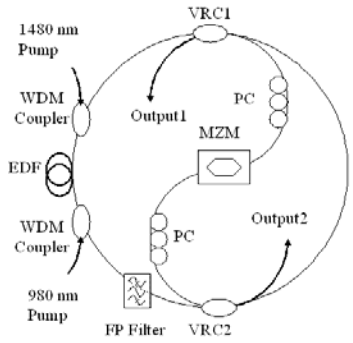

Fig. 10: Experimental setup for AM NOLM-NALM fiber laser (VRC – variable ratio coupler, PC – polarization controller, MZM – Mach Zehnder modulator)

V. Results and Discussion

A. *Bidirectional Erbium Doped Fiber Ring Laser*

The ASE spectrum of the laser covers the range from 1530nm to 1570nm. By increasing both the 980nm and 1480nm pumping currents to their maximum allowable values, we obtained bidirectional lasing, which is shown in Fig. 11. The upper plot is the lightwave propagating in the clock-wise direction while the other one in the opposite direction. The lasings of the laser in both directions are not very stable due to the disturbance from the opposite propagating lightwave and the ASE noise contribution due to the absence of filter. The Output1 is mainly contributed by the back reflections from the fiber ends and connectors, as well as some back-scattered noise.

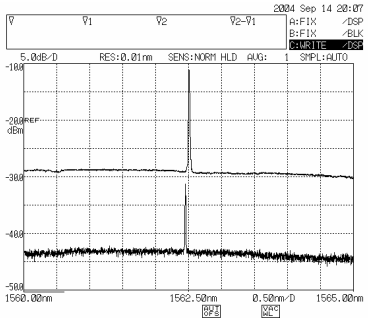

Fig. 11: Bidirectional lasing (upper trace: Output2; lower trace: Output1)

The optical bistable characteristics at a lasing wavelength of about 1562.2nm for both outputs directions are shown in Fig. 12. We obtained about 15dBm difference between the two propagating lightwaves. We maintain 980nm pump current at 100mA and adjust the 1480nm pump current upwards and then downwards to examine the bistability behavior of the laser. The bistable region obtained is about 30mA of 1480nm pump current at fixed 100mA 980nm pump current. No lasing is observed in the counter clockwise lightwave propagation.

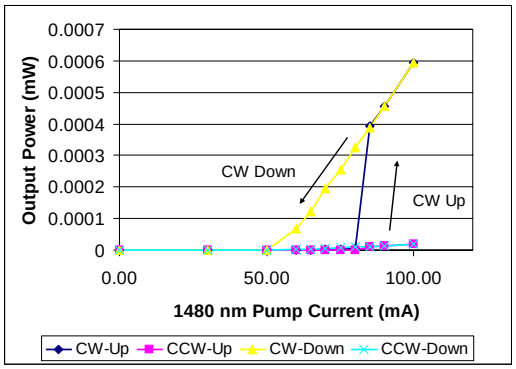

Fig. 12: Hysteresis loops obtained from the erbium-doped fiber ring laser (CW – clockwise; CCW – counter clockwise)

B. *NOLM-NALM Fiber Ring Laser*

One interesting phenomenon observed before the bandpass filter is inserted into the cavity is the wavelength tunability. The lasing wavelength is tunable from 1530 to 1560 nm (the entire EDFA C-band), by changing the coupling ratios of the VRCs. We believe this tunability is due to the change in the traveling wave power, which leads to the change in the dispersion relations of the cavity, hence the lasing wavelength. Thus, the VRCs within the cavity not only determine the directionality of the lightwave propagation, but also the lasing wavelength.

A small hysteresis loop has also been observed when changing the coupling ratio of one VRC while that of the other one remains unchanged, as shown in Fig. 13. Changing the coupling ratio of the VRC, is directly altering the total power within the cavity, and hence modifying its gain and absorption behavior. As a result, a small hysteresis loop is observable even with a constant pump power. The simulated optical bistabilty of the NOLM-NALM is shown in Fig. 14.

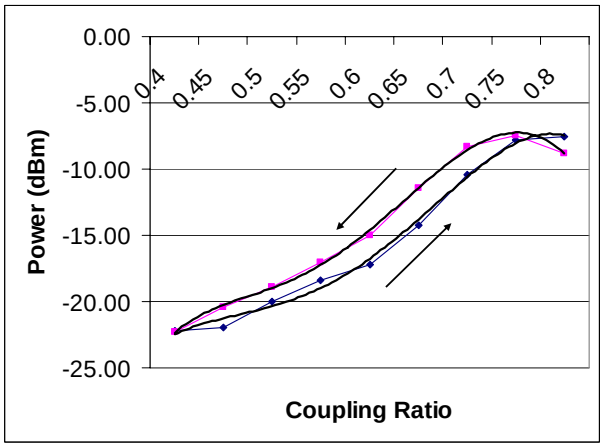

Fig. 13: Hysteresis observed while changing the coupling ratio of the VRC

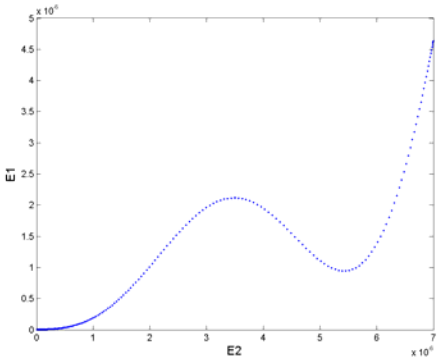

Fig. 14: Optical bistability observed in the NOLM-NALM laser

The power distribution of the Output1 and Output2 of the NOLM-NALM fiber laser is depicted in Fig. 15. We are able to obtain the switching between the Output1 and Output2 by tuning the coupling ratios of VRC1 and VRC2. The simulation results for various coupling ratios under linear operation are shown in Fig. 16, since the available pump power of our experiment setup is insufficient to create high power within the cavity. Both the results have come to some agreements, but not all, since the model developed is simple and does not consider the polarization, dispersion characteristics and etc. of the propagating lightwaves.

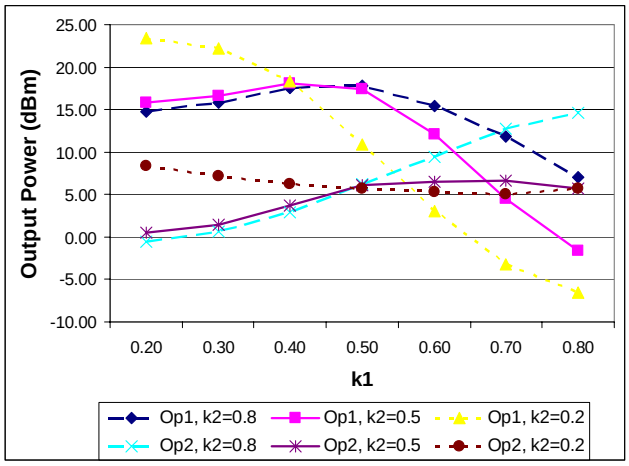

Fig. 15: Output powers for Output1 (Op1) and Output2 (Op2) for various coupling ratios (k1 – coupling ratio of VRC1, k2 – coupling ratio of VRC2)

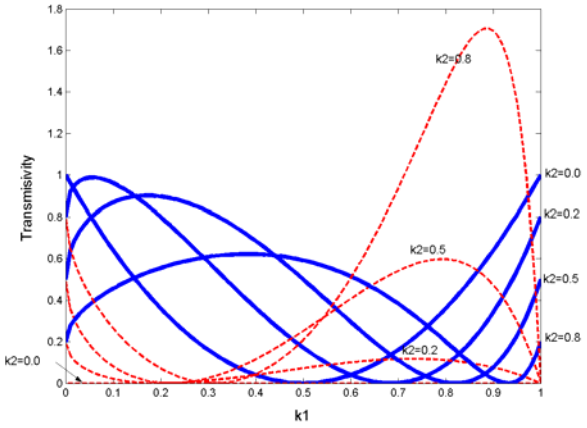

Fig. 16: Transmisivities of Output1 (solid line) and Output2 (dotted line) for various coupling ratios of VRC1 and VRC2

C. *AM Modulated NOLM-NALM Fiber Ring Laser*

With the insertion of the AM modulator into the laser cavity, we are able to obtain the pulse operation from the laser, by means of active harmonic mode-locking technique. Both propagation lightwaves are observed. By proper adjustment of the modulation frequency, the polarization controllers and the variable ratio couplers, unidirectional pulse operation at modulating frequency is obtained. However, it is highly sensitive to the environmental change. The direction of the lightwave propagation of the laser can be controlled by the VRCs. The unidirectional pulse train propagations obtained experimentally and numerically are shown in Fig. 17.

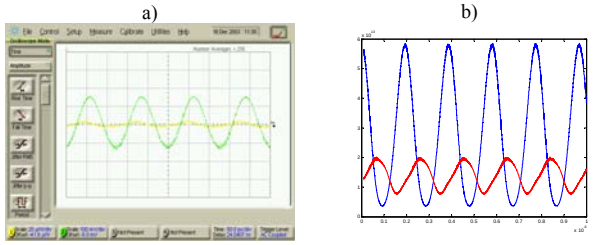

Fig. 17: Unidirectional pulse operation in AM NOLM-NALM fiber laser. (a) Experimental results; (b) simulation results

However, with slight deviations to the system parameters, period doubling and quasi-periodic operations in the laser are observed, as shown in Fig. 18. We believe that the effect is due the interference between the bidirectional propagations lightwaves, which have suffered nonlinear phase shifts in each direction, since we are operating in the saturation region of the EDFA. Another factor for this formation is that the lightwave in one direction is the feedback signal for another one. Furthermore the intensity modulation of the optical modulator is not identical for co- and counter- interactions between the lightwaves and the traveling microwaves on the surface of the optical waveguide. This would contribute to the mismatch of the locking condition of the laser.

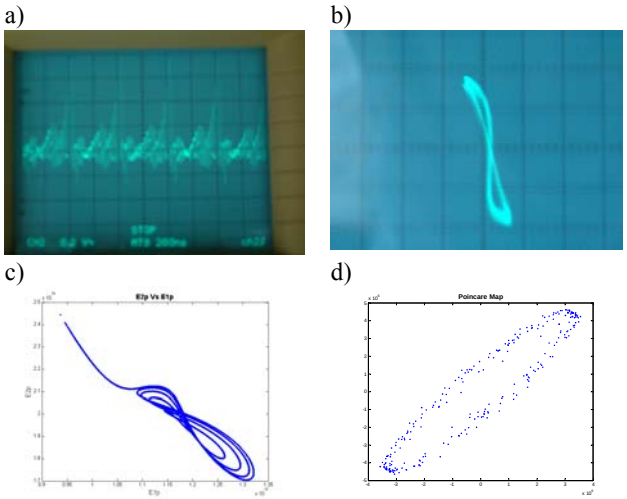

Fig. 18: Quasi-periodic operation in AM NOLM-NALM fiber laser; (a) photograph of the oscilloscope trace, (b) XY plot of Output 1 and 2, (c) simulated XY plot, (d) simulated Poincare map

VI. Conclusions

Bidirectional optical bistability in a dual-pumped erbium doped fiber ring laser without isolator has been studied. A ~70mA 1480 nm pump current bistable region has also been obtained. With this bidirectional bistability capability, we experimentally constructed and numerically simulated a NOLM-NALM fiber laser for switching operation. The VRCs used in the setup not only control the lightwave directionality, but also its lasing wavelength. Unidirectional lightwave propagations, without isolator, were achieved in both cw and pulse operations by tuning the coupling ratios of the VRCs within the laser system. Bifurcation was also obtained from the AM NOLM-NALM fiber laser. However, chaotic operation was not obtained experimentally due to the hardware limitation of our system, which required higher gain coefficient and input power as predicted in our simulation.

We foresee this NOLM-NALM fiber laser has potentials in many applications, such as photonic flip-flops, optical buffer loop, photonic pulse sampling devices, secured optical communications etc.

References

[1] A.E. Siegman, *Lasers*, Mill Valley, CA: University Science Books, 1986

[2] Y. Shi, M. Sejka and O. Poulsen, "A unidirectional Er^{3+} -doped fiber ring laser without isolator", IEEE Photonics Technology Letters, Vol. 7, No. 3, pp. 290-292, 1995

[3] N. J. Doran and D. Wood, "Nonlinear-optical loop mirror", Optics Letters, Vol. 13, No. 1, pp. 56-58, 1988

[4] M. E. Fermann, F. Haberl, M. Hofer and H. Hochreiter, "Nonlinear amplifying loop mirror", Optics Letters, Vol. 15, No. 13, pp. 752-754, 1990

[5] K. K. Gupta, N. Onodera and M. Hyodo, "Technique to generate equal amplitude, higher-order optical pulses in rational harmonically modelocked fiber ring lasers", Electronics Letters, Vol. 37, No. 15, pp. 948-950, 2001

[6] Y.D. Gong, P. Shum, D.Y. Tang, C. Lu, T.H. Cheng, Z.W. Qi, Y.L. Guan, W.J. Lai, W.S. Man and H.Y. Tam, "Bound solitons with 103fs pulse width and 585.5fs separation from DI-NOLM figure-8 fiber laser", Microwave and Optical Technology Letters, Vol. 39, No. 2, pp. 163-164, 2003

[7] W.J Lai, L.N. Binh, P. Shum and Y.D. Gong, "Ultra-stable multi-giga-pulses/sec fiber mode-locked generator", 2nd Conference on Optical Internet & 28th Australian Conference on Optical Fiber Technology, COIN/ACOFT, PO1-1.3, 2003

[8] M. Nakazawa, E. Yoshida, "A 40 GHz 850 fs regeneratively FM mode-locked polarization maintaining erbium fiber ring", IEEE Photonics Technology Letters, Vol. 12, No. 12, pp. 1613-1615, 2000

[9] G. Yandong, S. Ping, T.Dingyuan, '298 fs Passively Mode Locked Ring Fiber Soliton Laser', Microwave and Optical Technology Letters, Vol.32, No.5, pp. 320-333, 2002

[10] K.Tamura, E.P.Ippen, H.A.Haus and L.E.Nelson, '77-fs pulse generation from a stretched-pulse mode locked all fiber ring laser', Optics letters, Vol.18, No.13, pp. 1080-1082, 1993